$^{1}H/^{19}F$ MRI of histological tumor sections using a double tunable surface coil

Gunthard Lykowsky[1], Thomas Christian Basse-Lüsebrink[1], Thomas Kampf[2], Michael Hess[3], Stephanie Weibel[3], Aladar A. Szalay[4], Peter Michael Jakob[1,2], and Daniel Haddad[1]

[1]*Research Center for Magnetic Resonance Bavaria e.V., Würzburg, Bavaria, Germany,* [2]*Department for Experimental Physics 5, University of Würzburg, Bavaria, Germany,* [3]*Department of Biochemistry, University of Würzburg, Bavaria, Germany,* [4]*Genelux Corporation, San Diego, CA, United States*

Target Audience: ^{19}F MRI, cell tracking, tissue engineering and regenerative medicine communities

Purpose:

Within the last few years, ^{19}F MRI was successfully applied to numerous research questions including those focusing on pulmonary imaging using fluorinated gases[1], measurement of the partial oxygen pressure[2] and ^{19}F-based cell tracking[3,4]. Regarding ^{19}F-based cell tracking, *ex-vivo* MRI in combination with immunohistochemistry is often performed to validate *in-vivo* findings[4]. Unfortunately, due to different sample geometries and sizes, the correlation of the different imaging modalities is limited[4]. For ^{1}H MRI, coils optimized for imaging of histological samples have been successfully applied[5,6]. Using these coils, ^{1}H MRI images of histological samples could be obtained, allowing exact correlation of histological findings with MRI data. The current work expands the concept of ^{1}H MRI on histological tissue samples to $^{1}H/^{19}F$ MRI, thus allowing correlation between the $^{1}H/^{19}F$ MR data and histology.

Methods:

Tumor Model and In-vivo Labeling Procedure:

An attenuated oncolytic Vaccinia virus (strain GLV-1h68) was injected i.v. into a mouse bearing a subcutaneous 1936-MEL melanoma of 150 mm^3. Four days after GLV-1h68 injection, 100 µl of perfluoropolyether (PFC) emulsion was injected i.v.. As mentioned in[7], PFC emulsion nanoparticles are internalized by phagocytic cells (monocytes, macrophages). The tumor was excised 11 days post infection.

Experiment Procedure:

Fig.1A shows a sketch illustrating the preparation and measurement procedure. After freezing, fixation, rinsing, and embedding, the tumor was sectioned into 150 µm thick slides using a Vibratom. The sections were labeled with primary CD68 antibodies (monocytes, macrophages) and secondary Cy3-conjugated anti-rat antibodies and mounted on glass slides (Fig. 1A). More details of this preparation procedure can be found in[8,9]. In a second step, (fluorescence) microscopic images were obtained from an antibody-labeled tumor section (Fig. 1B). Finally, $^{1}H/^{19}F$ MR projection images were obtained from the same tumor section as used for fluorescence microscopy (Fig. 1C).

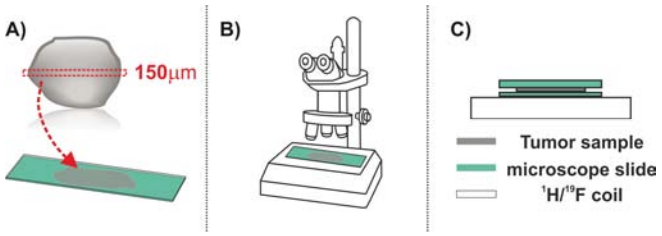

Fig.1) Simplified sketch illustrating the preparation and measurement procedure.
A) In a first step, the tumor was cut into tissue sections of 150 µm.
B) Second, immunohistochemistry was performed on the chosen tissue section.
C) Finally, ex-vivo *MRI was performed on the same tissue section as used for immunohistochemistry.*

MRI:

For MRI, a customized double-tunable $^{1}H/^{19}F$ surface coil was built (2 cm side length). Similar coils have been shown to deliver a high sensitivity and sufficient in-plane B_1 homogeneity to perform MRI on histological slices[6]. Imaging of the tumor slice was performed using a 7T small animal scanner. ^{1}**H** imaging parameters: Sequence = Multi spin echo, TIE/TR = 9/1000ms, Res = 0.1x0.1mm^2, NA = 16. ^{19}**F** imaging parameters: Sequence (low-resolved) = Turbo spin echo (TSE), TE/TR = 6.2/1000ms, Res = 0.4x0.4mm^2, TF = 48, NA = 3600; Sequence (high-resolved) = TSE, TE/TR = 6.3/1500ms, Res = 0.12x0.1mm^2, TF = 64, NA = 14400.

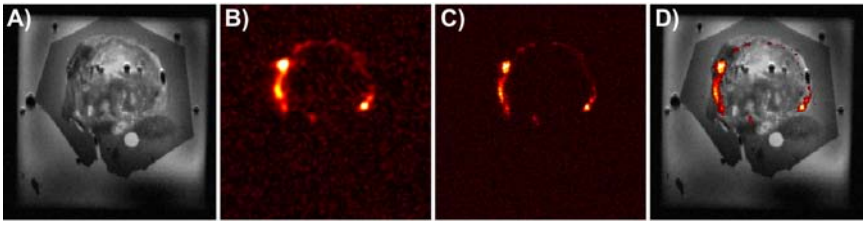

Fig.2) MRI results. A) ^{1}H Image (TE = 18ms). B) ^{19}F MRI (low-resolved). C) ^{19}F MRI (high-resolved). D) $^{19}F/^{1}H$ overlay (high-resolved ^{19}F MRI data).

Results:

Fig.2 shows the MRI results. High-resolved ^{1}H MRI data as well as low- and high-resolved ^{19}F data were obtained. The ^{1}H MRI data and the low-resolved ^{19}F MRI data were both obtained in approximately 1h measurement time (Fig. 2A and B). The high-resolved ^{19}F MRI data were obtained in 24 h (Fig.2C). The $^{19}F/^{1}H$ overlay in Fig.2D shows that the ^{19}F signal was restricted to the tumor margin.

Fig.3 presents the histology results. In Fig.3A, a top-light image of the tumor section is shown. The green GFP signal in Fig.3B shows tumor cells infected by the VACV virus, which were distributed throughout the tumor. Furthermore, signal originating from CD68-positive cells was located at the tumor margin. Correlation of the histological and the ^{19}F MRI data revealed a similar distribution pattern between the ^{19}F signal and the CD68 signal (Fig.3C and 3D).

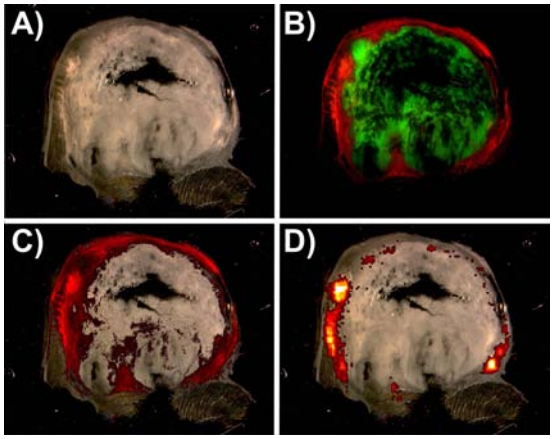

Fig.3) Histology results. A) Top-light tumor image. B) Immunohistochemistry: Red: CD-68, Green: GFP. C) CD-68 positive cells/ tumor image overlay. D) ^{19}F MRI/tumor image overlay (high-resolved ^{19}F MRI data).

Discussion and Conclusion:

Using an optimized $^{1}H/^{19}F$ surface coil, the ^{19}F signal distribution in a thin tumor section was obtained in acceptable measurement times. Since the same section was measured using both fluorescence-microscopy and MRI, a correlation of the MRI findings with histology was enabled. Thus, in the future this technique can improve the validation of *in-vivo* MR findings. Furthermore, markers visible in both microscopy and MRI could further enhance data correlation.

In this proof-of-principle study, a single, small $^{1}H/^{19}F$ surface coil was used. Since only one tumor section could be investigated per measurement session using this setup, investigating the entire tumor would be a time consuming process. In the future, double-resonant coil arrays might overcome the limitation of single coils, thus allowing simultaneous measurement of multiple tissue sections.

References:

[1] Adolphi et al. (2008), Mag. Reson. Med. 59
[2] Giraudeau et al. (2012), NMR Biomed. 25
[3] Srinivas et al. (2009), Mag. Reson. Med. 62
[4] Weibel et al. (2013), PloS One. 8
[5] Meadowcroft et al. (2007), Magn Reson Med 57
[6] Nabuurs et al. (2011), NMR Biomed. 24
[7] Temme et al. (2012), WIREs N Nanobiotechnol. 4
[8] Weibel et al. (2008), Cellular Microbiology. 10
[9] Weibel et al. (2011), BMC Cancer. 11

Acknowledgements:

This work was supported by grants from Genelux Corporation (R&D facility in San Diego, CA, USA). AAS is a salaried employee of Genelux.